Paper No.
65—FE-3

Experimental Observations on the Flow Past a Plano-Convex Hydrofoil

R. B. WADE
Graduate Research Assistant,
Division of Engineering and
Applied Science,
California Institute of Technology,
Pasadena, Calif.

A. J. ACOSTA
Associate Professor of
Mechanical Engineering,
Division of Engineering and
Applied Science,
California Institute of Technology,
Pasadena, Calif. Mem. ASME

Some new measurements and observations on the noncavitating and cavitating flow past a plano-convex hydrofoil are presented. Under some conditions of partial cavitation, strong, periodic oscillations both in the cavity length and forces exerted on the hydrofoil are observed. The reduced frequency of oscillation depends upon the cavitation number and angle of attack; it also depends somewhat on tunnel speed for the lower angles of attack but becomes substantially independent of speed for the highest angle. The peak-to-peak magnitude of the force oscillation can amount to about 20 percent of the average force.

Introduction

With the advent of the hydrofoil boat and the demand for higher speed pumps and propellers, a detailed knowledge of the performance of hydrofoil sections under all conditions of cavitation becomes necessary for the proper understanding of events that may occur in engineering applications. We have been interested for some time in the cavitating flow through hydrofoils arranged in cascade because of its obvious application to pumps and perhaps propellers. In considering possible hydrofoil profile shapes for such experiments, we settled upon a plano-convex shape (flat bottom and circular arc upper surface) for its simplicity and economy of manufacture and also because extensive use is made of slight variants from this form for propeller sections. An added but not essential consideration is that analytic calculations are facilitated by a simple geometry.

As a preliminary step to the undertaking of a full-scale cascade experiment, we decided to study the characteristics of an individual foil of the type chosen as this would suggest possible phenomena to look for in cascade. Also, because of the greater difficulty of experimentation, it was not likely that the performance in cascade could be examined in as great detail as that of an isolated hydrofoil. Furthermore, such tests are in themselves of considerable interest. Experimental studies on plano-convex profiles or on closely related ones are, however, not new. Balhan [1],[1] for example, reports cavitation experiments made on a series of Karman-Trefftz profiles. Experiments on a similar section were made by Walchner [2] and more recently by Kermeen [3]. Generally, the profiles of these studies differ from the present one in certain respects—notably the leading edge detail—except for [1], in which the extent of cavitation is much less than that of the present work.

Plano-convex hydrofoils, like the other members of the Karman-Trefftz series, have sharp leading and trailing edges. At positive angles of attack, an infinitely negative pressure occurs at the leading edge and normally a cavity would be expected to spring from the leading edge. This, however, does not always occur. At low angles of attack, below 4 deg for the section tested, the cavity appears downstream of the leading edge on the low-pressure surface. In fact, for some of these lower angles, two cavities are observed simultaneously; one, very short, springing from the leading edge and the other from a point near the maximum thickness of the hydrofoil. At and above 4 deg, the cavity starts at the leading edge for all conditions of cavitation; and in the present work, the emphasis is placed on angles of attack greater than 4 deg. The cavity-detachment point is thus fixed at the leading edge in the range tested, resulting in a more readily anticipated flow pattern and a more straightforward interpretation of the experimental results than otherwise would have been the case. One outcome of this restriction is that the profile becomes a flat plate for cavities longer than the chord, a configuration already tested by Parkin [4].

Description of Experiments

Measurements of the lift force, drag, and moment on the hydrofoil were made with no cavitation to determine this basic flow. Cavitation experiments were then carried out by fixing the angle of attack and lowering the tunnel pressure. The object of these experiments was to determine the performance of the hydrofoil under cavitating conditions, i.e., lift, drag, and so on, and to observe the formation and development of the cavitation or two-phase region formed about the hydrofoil. Of special interest here was the measurement of cavity lengths. Under some conditions, however, the cavity on the hydrofoil oscillated with a recognizable period; it was also clear from the vibrations of the tunnel apparatus and structure that there were considerable fluctuations of the forces on the hydrofoil as well. A number of experiments of a preliminary nature were carried out to ascertain the magnitude of the forces and associated frequencies. For this purpose, a few moderately high-speed 16-mm motion-picture

[1] Numbers in brackets designate References at end of paper.

Contributed by the Fluids Engineering Division for presentation at the Applied Mechanics/Fluids Engineering Conference, Washington, D. C., June 7–9, 1965, of The American Society of Mechanical Engineers. Manuscript received at ASME Headquarters, February 19, 1965. Paper No. 65—FE-3.

Nomenclature

A = plan form area = $(s \times c)$
c = chord length
C_D = drag coefficient = $\dfrac{D}{A\rho V^2/2}$
C_L = lift coefficient = $\dfrac{L}{A\rho V^2/2}$
C_M = moment coefficient $\dfrac{M}{Ac\rho V^2/2}$ about the midchord point
D = drag force on model
f = frequency of oscillations
K = corrected cavitation number = $\dfrac{p - p_k}{\rho V^2/2}$
K_v = cavitation number based on vapor pressure = $\dfrac{p - p_v}{\rho V^2/2}$
l = cavity length
L = lift force on model
M = moment on model
p = corrected tunnel static pressure
p_k = measured cavity pressure
p_v = vapor pressure of water
R = radius of circular surface of model
s = span
t = thickness of hydrofoil
V = tunnel velocity
α = angle of attack, degrees measured from chord line
λ = distance of center of pressure from leading edge
ρ = density of water

sequences were made. An Eastman camera was used and the average frame speed was about 1900 per sec. The development of cavities is, of course, of great interest; but of particular importance for the present problem is the relationship between the geometry of the growing and collapsing cavitation pattern and the variation of the force on the cavity. For this purpose, the high-speed *motion* pictures recorded the output of a strain gage mounted on the hydrofoil simultaneously with the cavity motion. Several film strips were assembled into a short sound motion picture[2] which illustrates this nonsteady cavitation process.

This unsteady cavitation phenomenon has been noted before in reference [4] and also by Meijer [5], who carried out similar experiments on very thin hydrofoils. Observations on the frequency and amplitude of these oscillations do not seem to have been reported as yet although a somewhat similar phenomenon has been described by Knapp [6]. In his experiments, partial cavitation was observed on hemisphere-cylinder bodies of revolution and thick, two-dimensional, nonlifting bodies consisting of a flat plate with a half-round circular nose.

Experimental Procedure

The tests were conducted in the high-speed water tunnel at the Hydrodynamics Laboratory [7]. The test model used, as previously mentioned, was a plano-convex hydrofoil, the dimensions of which are shown in Figs. 1 (*a*) and 1 (*b*). The leading and trailing edges of the hydrofoil were left perfectly sharp. The 14-in-dia cylindrical section of the tunnel was converted to an approximately 14-in. by 3-in. two-dimensional rectangular section by the use of inserts, as explained in [3].

The model was integrally machined with the base plate shown in Fig. 1 (*a*) which was bolted to the spindle of the force balance. Shims were used so that the plate was made flush with the tunnel wall. A circular gap of approximately 0.020 in. was left between the model attachment piece and the surrounding tunnel wall. The force balance and readout equipment which were used to measure the steady values of lift, drag, and moment on the hydrofoil were the same as in [3]. A detailed description of the force-measuring equipment is given in [8].

Normally, two kinds of experiments were made for the steady forces. Fully wetted data were obtained at constant tunnel speed and pressure, and the angle of attack was varied over the region of interest, in the present case −4 to 15 deg angle of attack with increments of 15 min of arc. This was repeated for several velocities to give a range of Reynolds numbers. Cavitation experiments, however, were made with a constant angle of attack and the ambient pressure within the tunnel varied to obtain the full range of cavitation. These tests covered a range of angles of attack of 4 to 10 deg and velocities from 15 to 40 fps.

The experimental setup is shown in Fig. 2. Two of the force-measuring balances are shown in this illustration, as well as the recording cameras. For both cavitation and fully wetted measurements, 35-mm cameras were used to record the readings of the force console. Additional cameras were also used to record, simultaneously with the force measurements, elevation and plan form views of the cavitation on the hydrofoil. The lengths of cavities were measured from these photographs.

The end gap between the model and the facing wall of the two-dimensional test section was adjusted to 0.005 in. and kept approximately at this value throughout the experiment. Although the end gap did vary slightly throughout the experiment, it was found that the variation of the forces with end gap for fully wetted flows over a range of 0.005 to 0.0105 in. was less than 5 percent for the lift and drag and negligible for the case of moment. During a test run, the variation of the end gap was never greater than 0.004 in.; hence this effect was sufficiently small to be considered negligible. Similar results were obtained in [3], although a somewhat larger drag variation was obtained there probably because of the greater thickness of the model.

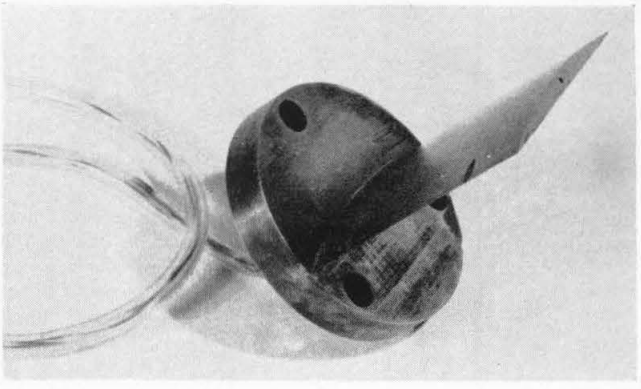

Fig. 1(a) Model and base plate

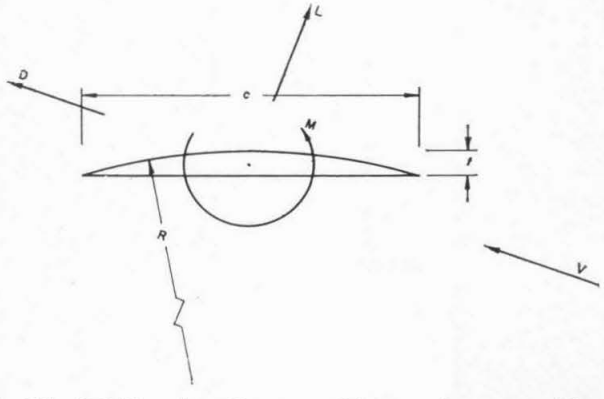

Fig. 1(b) Definition of positive sense of forces and moments. Dimensions of model used are C = 2.77 in., t = 0.19 in., R = 5 in., s = 2.85 in.

The readings of the force gages were corrected for tunnel static-pressure interactions and for the tare forces on the mounting disk. These tare forces, although small in the case of lift and negligible in the case of moment, comprise, under certain circumstances, as much as 30 percent of the total drag force. The details of the tare-force determinations and the method of obtaining these results, by mounting the model from the opposite wall of the tunnel, are described in [3].

The dynamic head $\rho V^2/2$, and hence the tunnel speed V, was determined by measuring the pressure drop between the piezometer ring at the 5-ft-dia circular section of the tunnel upstream of the tunnel nozzle and the two-dimensional section itself. This pressure difference was recorded on the force read-out console. The static pressure in the tunnel was measured at the two-dimensional section by means of a mercury manometer.

The difference between the working-section static pressure and the pressure within the cavity was measured with a mercury manometer. The cavity-pressure orifice was located 0.2 in. behind the leading edge on the suction face of the hydrofoil at midspan. Owing to the frothy nature of the cavity, water tended to enter the tubing connecting the cavity orifice with the manometer, thus causing false readings. To insure a correct reading of the cavity pressure at all times, this line was kept clear of water by constant purging with a small amount of bleed air.[3] The resulting error in pressure was always less than 0.8 in. of water, which

[2] The film, entitled "Some Non-Steady Effects in Cavity Flows," Report No. E-79.6, may be borrowed from the Hydrodynamics Laboratory, Karman Laboratory of Fluid Mechanics and Jet Propulsion, California Institute of Technology, Pasadena, Calif.

[3] This portion of the work was carried out before the work of G. Gadd, "An Air-Blowing Technique for Measuring Pressures in Water," National Physical Laboratory Report SH.R24/61, 1961, was available. The present method, essentially the same as Gadd's, was devised by T. Kiceniuk.

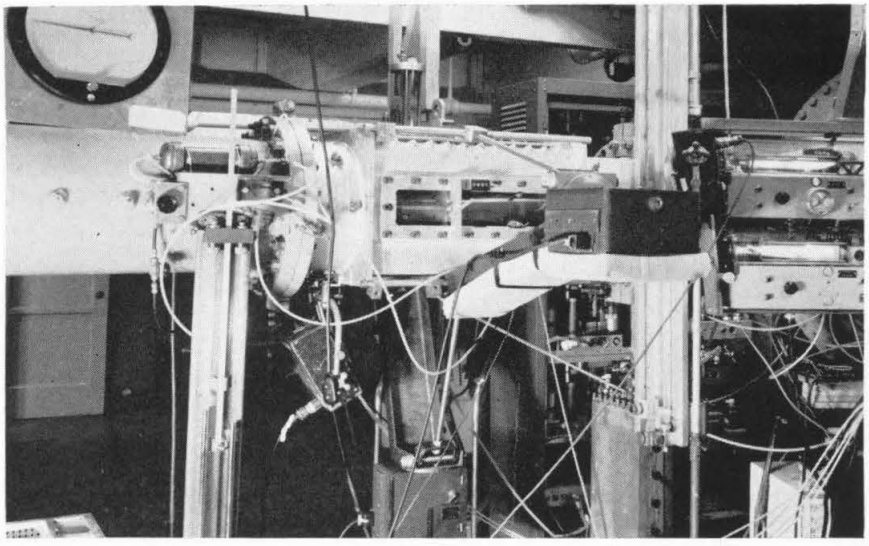

Fig. 2 Tunnel working section together with manometers and recording cameras

corresponds to an error in the determination of cavitation number of about 1 percent or less in the worst case.

The present working section presents severe limitations in the measurement of the relevant pressures that are needed to present the results in useful form. It is frequently impractical to have a two-dimensional section of sufficient length to measure the static pressure that would prevail an infinite distance upstream, even though this is what is needed in the reduction of force coefficients, and so forth. In the present case, the static pressure in the working section was measured at an orifice $2^1/_4$ chords upstream of the midpoint of the hydrofoil and 1.4 chords above the level of the hydrofoil. However, a different orifice only 1.8 chords from the model center line and on the center line of the flow was used as the working-section, static-pressure reference for the measurement of cavity pressure. Both orifices are sufficiently close to the hydrofoil so that it can be anticipated that the pressures there will be noticeably affected by the lift force and possibly by the cavity size.[4] As all force coefficients and cavitation indexes are based on the working-section pressure, it is necessary that the foregoing effects be taken into account. Therefore, an extensive tunnel calibration was carried out to provide this information. The appropriate details can be found in [10]. Briefly, the procedure was to use, as a calibrating pressure orifice, a point nearly midway between the test section and the upstream inlet to the nozzle. Then, presuming the influence of forces on the hydrofoil not to affect this pressure, the ratio of the pressure differences between the tunnel total pressure and the various points in question was determined for various values of lift, drag, and cavitation number. This procedure is nearly the same as that used by Kermeen in making his measurements.

As previously mentioned, experiments were made to measure the force variations on the hydrofoil during the nonsteady cavity oscillations. The force balance used to measure the steady forces was entirely too massive to respond to these rapid fluctuations. Visual observation of the flow with a "Strobotac" indicated that the frequencies could vary from about 10 to 30 cps. To study this region more thoroughly, therefore, it was necessary to employ transducers of moderately fast response. At the same time, it was realized that it would be expensive to manufacture a three-component, fast-responding force balance for these preliminary tests. To get a measure of the fluctuating forces and to measure the frequencies more accurately than could be done with a Strobotac, we flush-mounted a semiconductor, half-bridge strain gage at the root of the hydrofoil. The strain gage was located at

[4] The recent calculation of Fabula [9] shows that the effect of the cavity can be very important in the measurement of tunnel static pressure by the direct means chosen here.

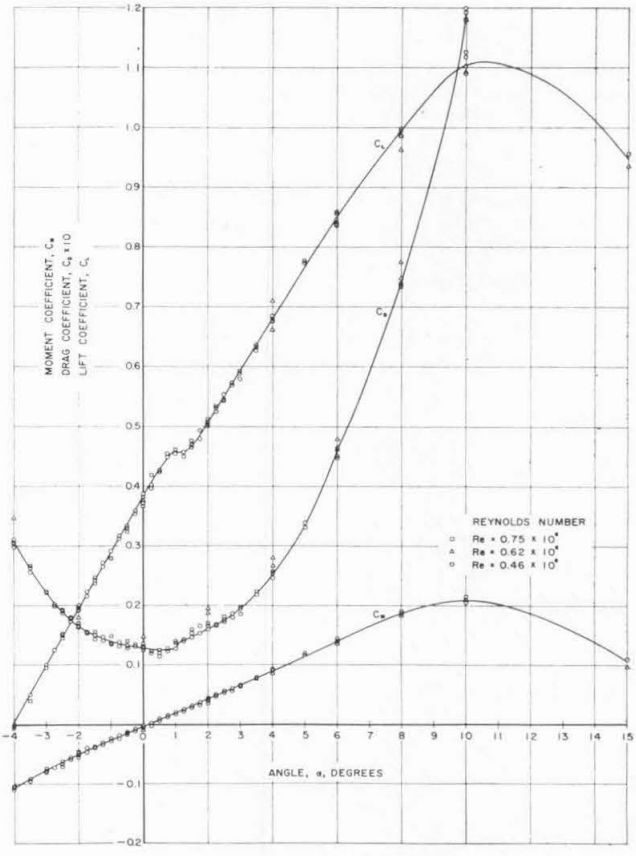

Fig. 3 Force coefficients as functions of angle of attack for noncavitating flow at several Reynolds numbers for plano-convex hydrofoil

the center of the hydrofoil and was waterproofed with the bonding agent used, a form of epoxy cement.

The output of the strain gage was recorded with a direct writing-recording oscillograph. No attempt was made to analyze separately the effects of moment, drag, and lift force on the output of the gage. It was assumed that the output would be proportional to the lift force and that this proportionality would be the same for static as well as dynamic conditions. For purposes of the present experiment, these assumptions seem reasonable. The strain

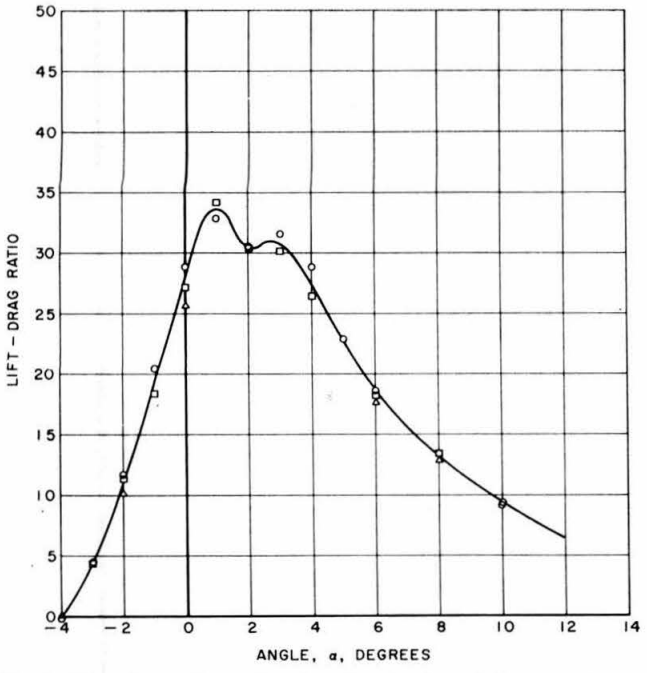

Fig. 4 Lift-to-drag ratio as a function of angle of attack for noncavitating flow at same Reynolds numbers indicated in Fig. 3

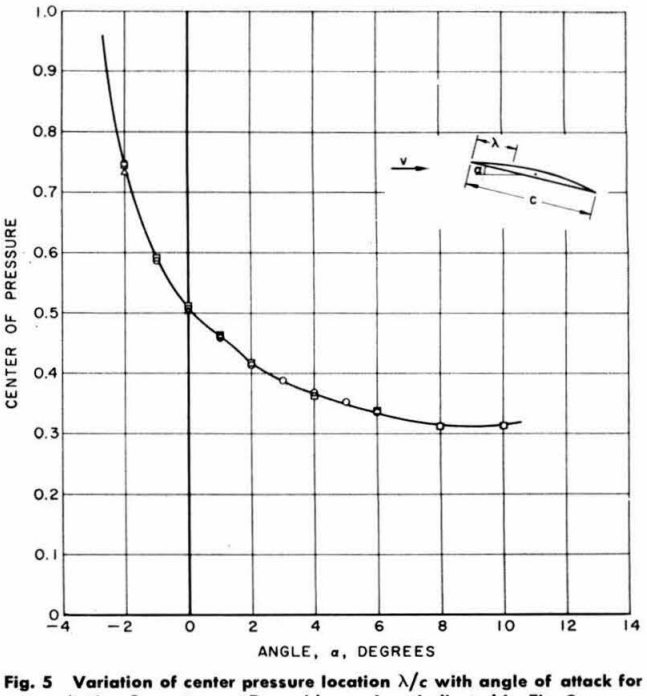

Fig. 5 Variation of center pressure location λ/c with angle of attack for noncavitating flow at same Reynolds numbers indicated in Fig. 3

gage was then calibrated by comparing its output with the output of the external force balance when the flow was steady.

Experimental Results

For each data point, lift, drag, and moment coefficients were calculated. No corrections were made for tunnel interference effects such as wall blockage, wake blockage, and longitudinal pressure gradient. All these effects are small for the present experiment except possibly for the fully cavitating flow.

Let us consider the fully wetted characteristics of the hydrofoil. In Fig. 3, the lift, drag, and moment coefficients are plotted versus angle of attack. The points are shown for a Reynolds number range of from 0.46×10^6 to 0.75×10^6 based on chord. Over this range, there is very little significant change in any of the force coefficients.

It is seen that at about 1 deg angle of attack, there is a slight stalling effect in the lift curve with a corresponding increase in the drag. This effect is characteristic of certain sharp-nose aerofoils and is due to the type of boundary-layer separation occurring on the foil [11, 12, 13]. This "wave" in the lift curve comes about because of the type of laminar separation of the boundary layer at the leading edge and its subsequent turbulent reattachment. This hump in the lift curve can be removed by increasing the Reynolds number to approximately 6×10^6 or by increasing the nose surface roughness. These effects are discussed in detail in the foregoing references. The lift slope is somewhat less than 2π below the hump and decreases further above it.

Figs. 4 and 5 show, respectively, the variation of the lift-to-drag ratio and the center-of-pressure location with angle of attack, the kinks in these curves being due, once again, to the boundary-layer separation.

To determine how consistently the cavity pressure, or cavitation number, could be recorded and how this reading compared with that based on vapor pressure, a plot of K against K_v was made for varying velocities and angles of attack. As seen in Fig. 6, this reading is quite repeatable. The discrepancy between the two readings increases with increasing cavitation number. It will be noted that the cavity pressure is always higher than the vapor pressure. This result is to be expected as the gases in solu-

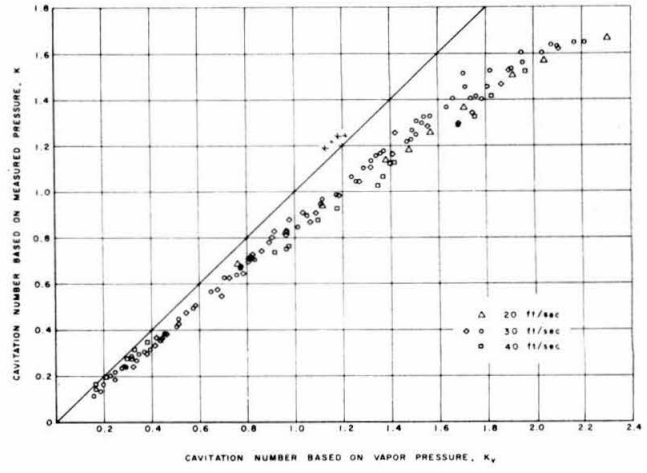

Fig. 6 Comparison of measured cavitation number to that based on vapor pressure

tion contribute to the pressure within the cavity. These results also check with those obtained previously [3].

For cavitating flow, the values of the force coefficients as a function of the measured cavitation number are shown in Figs. 7–10, each graph being for a different angle of attack. The subsequent photographs indicate the degree of cavitation occurring on the hydrofoil at a few different cavitation numbers which are marked on the graphs.

Figs. 11–14 show graphs of the cavitation number divided by angle of attack as a function of cavity length. These points were obtained from the 35-mm photographs taken of the cavity for each data point. The solid points are those occurring in the unsteady flow regime. As can be seen, the unsteady region occurs over a region of approximately 0.6 l/c to 1.2 l/c, regardless of angle of attack. This region of unsteadiness is indicated on the graphs of the force coefficients as well. Here the forces are fluctuating violently, and the points shown plotted are "average" forces recorded by the balance. Although we believe these average forces are representative of the true time average, no systematic investigation of this point has yet been made.

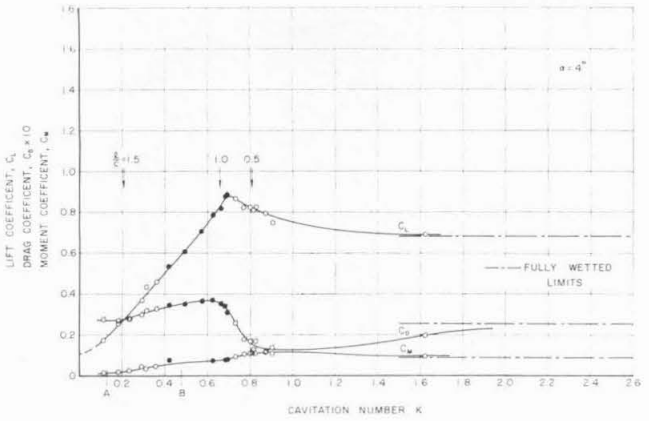

Fig. 7(a) Force coefficients as functions of cavitation number at an angle of attack of 4 deg for a plano-convex hydrofoil of 7 percent thickness. Note that all drag points are flagged.

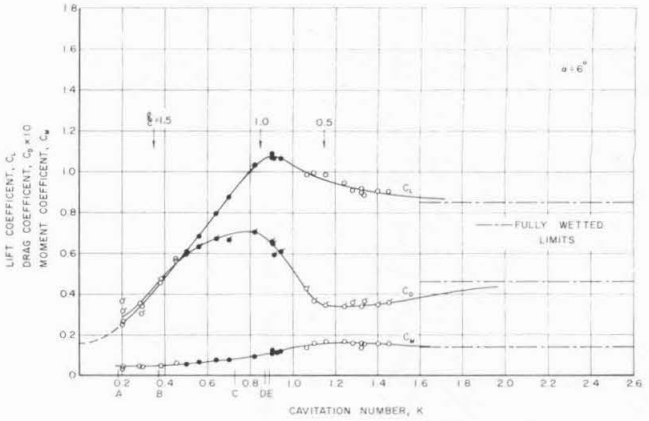

Fig. 8(a) Force coefficients as functions of cavitation number at an angle of attack of 6 deg for a plano-convex hydrofoil of 7 percent thickness. Note that all drag points are flagged.

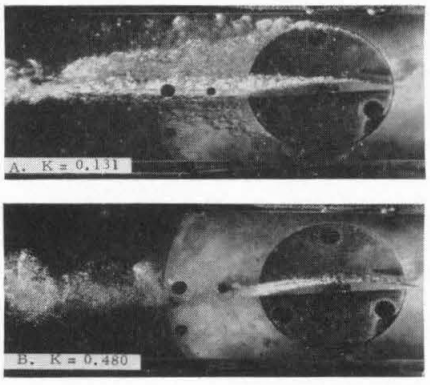

Fig. 7(b) Cavitation occurring on a plano-convex hydrofoil at an angle of attack of 4 deg at various cavitation numbers, K. Letters are those referred to in Fig. 7(a).

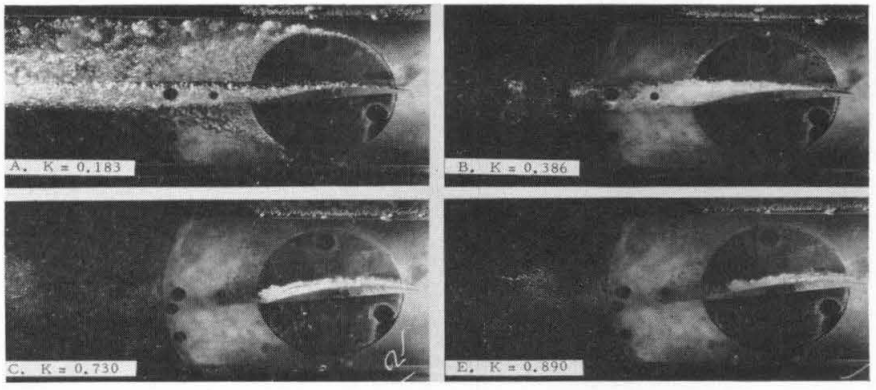

Fig. 8(b) Cavitation occurring on a plano-convex hydrofoil at an angle of attack of 6 deg at various cavitation numbers, K. Letters are those referred to in Fig. 8(a).

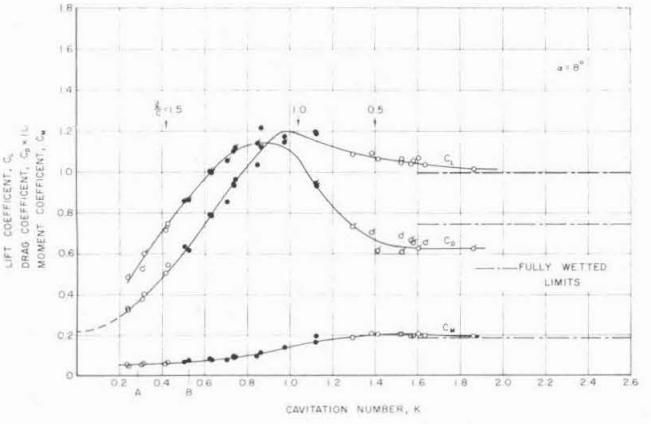

Fig. 9(a) Force coefficients as functions of cavitation number at an angle of attack of 8 deg for a plano-convex hydrofoil of 7 percent thickness. Note that all drag points are flagged.

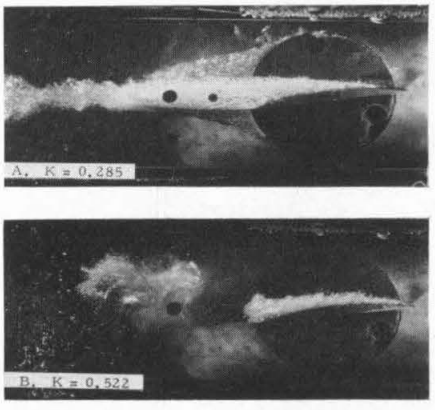

Fig. 9(b) Cavitation occurring on a plano-convex hydrofoil at an angle of attack of 8 deg at various cavitation numbers, K. Letters are those referred to in Fig. 9(a).

Theoretical curves obtained from linearized free-streamline theory in the regions of full cavitation [14] and partial cavitation [15] on a *flat-plate* hydrofoil are also shown in Figs. 11–14. We see that for fully cavitating flow the agreement is better than for the partial cavitating case. This, however, is to be expected since, in the former case, the hydrofoil acts exactly like a flat plate whereas, in partial cavitation, camber and thickness effects play a role.

Experimental results on a similar section are reported in [2] for noncavitating and cavitating conditions for angles of attack up

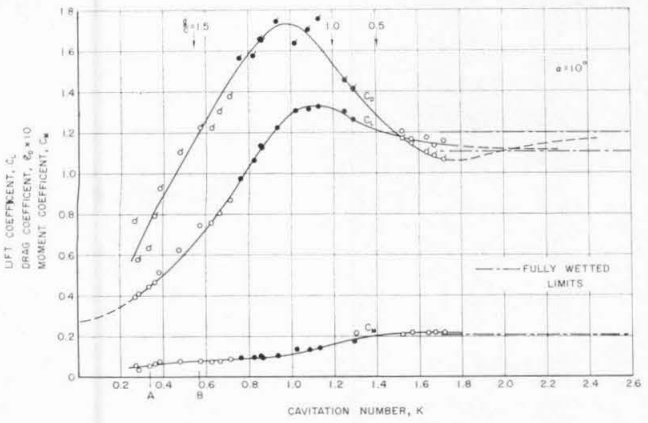

Fig. 10(a) Force coefficients as functions of cavitation number at an angle of attack of 10 deg for a plano-convex hydrofoil of 7 percent thickness. Note that all drag points are flagged.

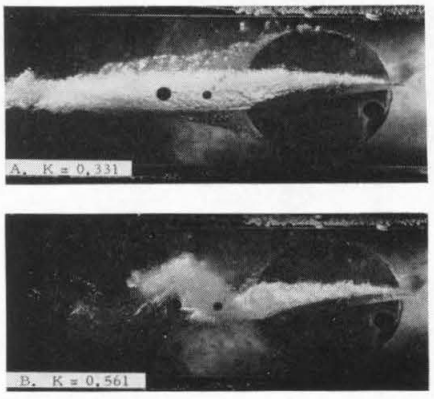

Fig. 10(b) Cavitation occurring on a plano-convex hydrofoil at an angle of attack of 10 deg at various cavitation numbers, K. Letters are those referred to in Fig. 10(a).

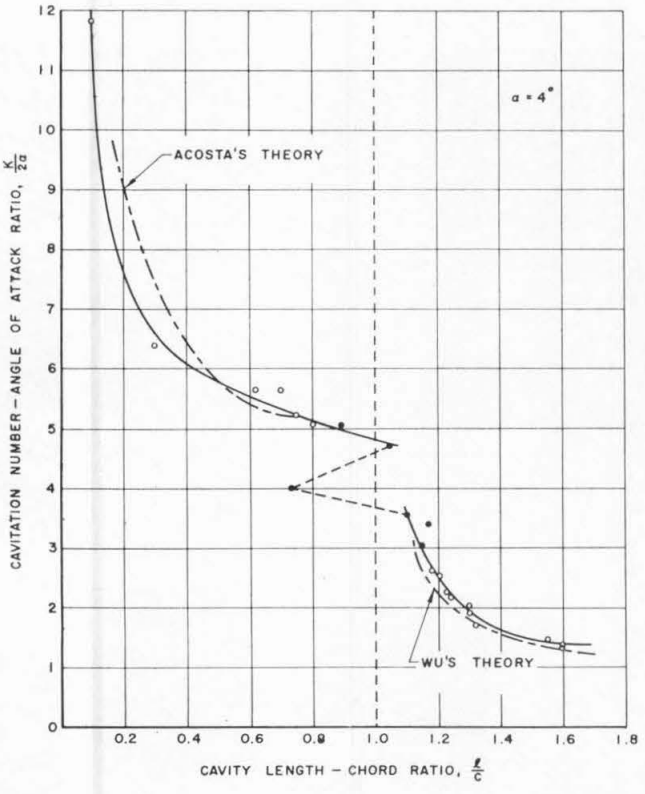

Fig. 11 Cavitation number divided by angle of attack as a function of cavity length-to-chord ratio for a plano-convex hydrofoil at an angle of attack of 4 deg

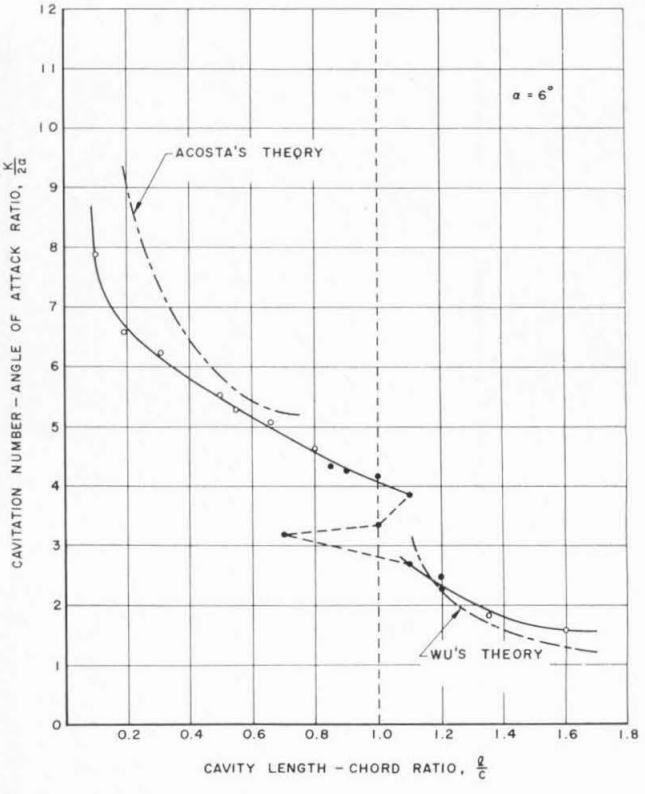

Fig. 12 Cavitation number divided by angle of attack as a function of cavity length-to-chord ratio for a plano-convex hydrofoil at an angle of attack of 6 deg

to 5 deg. The cavitation number in these experiments is based on vapor pressure and, hence, a direct comparison with the present data cannot be made exactly, and the thickness of the profile is slightly different. Nevertheless, quite a favorable agreement is found in the common region covered by both investigations.

Nonsteady Cavitation

As mentioned previously, oscillations in cavity length and hydrodynamic force developed when the cavity was about 60 percent or so of the chord and persisted until the cavity was at least 1.2 times the chord. A description of the development of this process now seems in order. The general behavior for all angles of attack equal to or greater than 4 deg is similar, and the general development of the nonsteady process is the same for all angles.

From the fully wetted condition to a cavity length of 60 percent chord, the cavities are steady in the mean; the cavity is not glassy clear, however, but is filled with a frothy mixture of air and water and has no definite structure, such as a reentrant jet, for example. Incidentally, at the very first stages of cavitation when the cavities are not longer than 2–3 percent of the chord, a relatively high-pitched oscillation and noise develop with a frequency of about 270 cps. This is thought to be associated with one of the fundamental vibratory modes of the hydrofoil itself. Although audible noise is generated, the resulting force oscillations are small as measured by the embedded strain gage. The cavity retains its

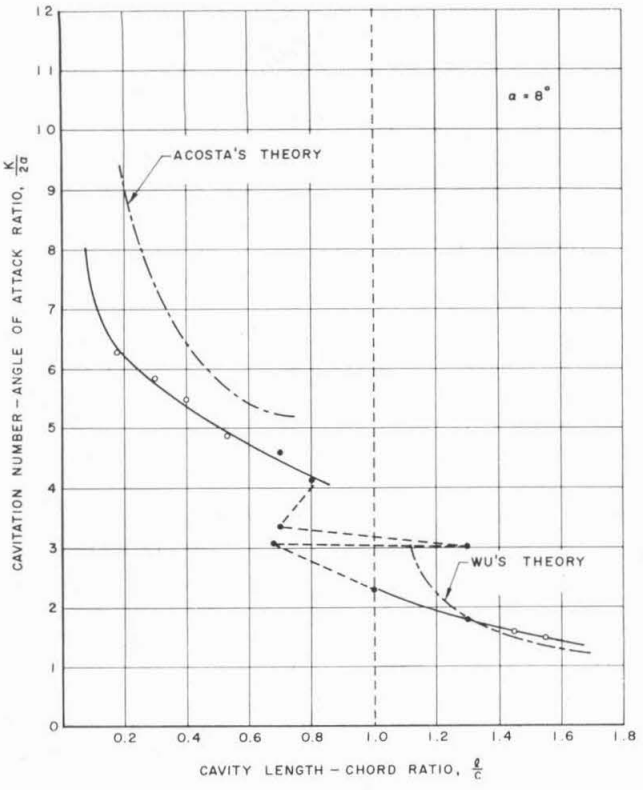

Fig. 13 Cavitation number divided by angle of attack as a function of cavity length-to-chord ratio for a plano-convex hydrofoil at an angle of attack of 8 deg

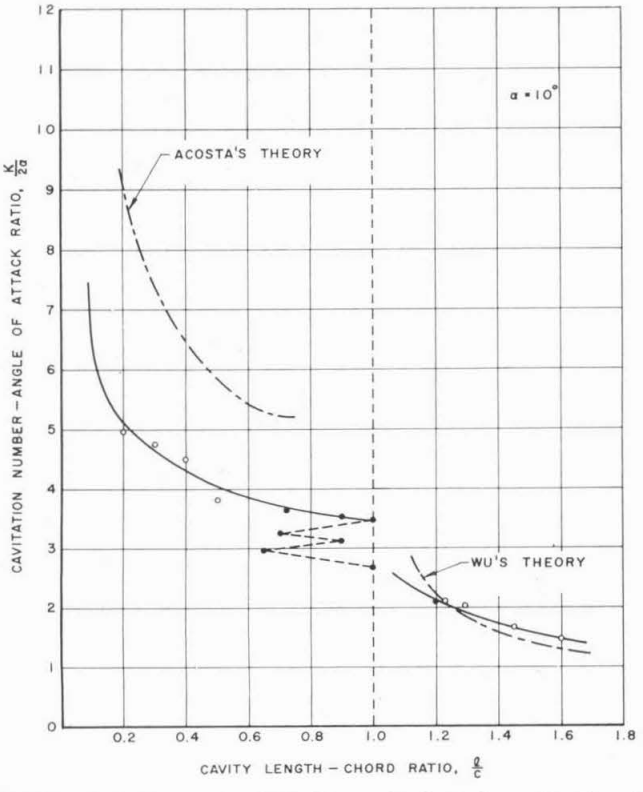

Fig. 14 Cavitation number divided by angle of attack as a function of cavity length-to-chord ratio for a plano-convex hydrofoil at an angle of attack of 10 deg

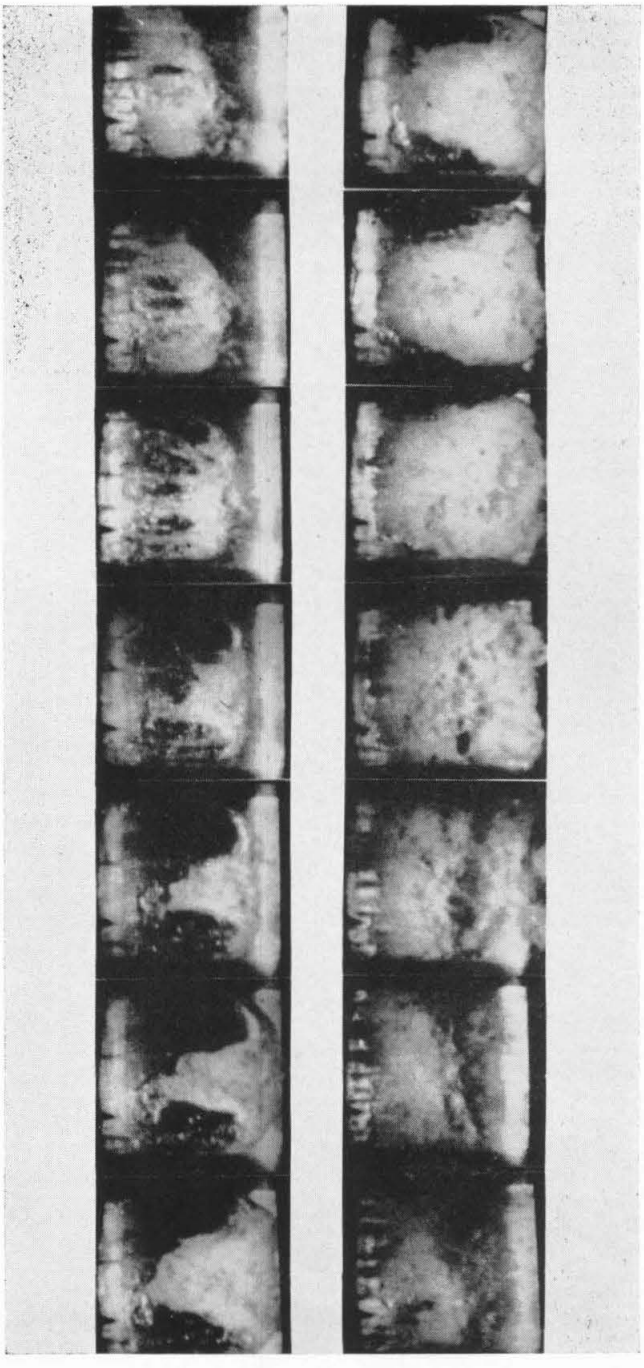

Fig. 15 This sequence of photographs shows in plan view behavior of cavity during one cycle of oscillation beginning with top left-hand view and proceeding down each column. Flow is from left to right, at a tunnel speed of 27 fps, with leading edge of plano-convex hydrofoil to left in each case. Angle of attack is 6 deg and cavitation number 0.90. Time lapse between each photograph is 0.0042 sec.

frothy character until just before oscillation commences, at which point the portion of the cavity near the leading edge becomes clear and glassy. Shortly thereafter, the cavity begins to oscillate. These initial oscillations are of small magnitude, both in extent and force, and are relatively high in frequency. For the present tunnel conditions, these frequencies may range from 50–60 cps. This stage of oscillation seems to be rather transitory; and with a slight decrease in tunnel pressure, the oscillation changes over into a more characteristic low-frequency, large-amplitude dis-

turbance. The oscillations then typically have a double amplitude of about one half chord. Typical frequencies in this stage under the conditions of our tests were about 12 to 25 cps depending upon velocity and angle of attack. The oscillations persisted with further lowering of tunnel pressure until the cavity was about one fourth longer than the chord. Generally, the amplitude of the cavity and force oscillation decreased. The flow then became quite steady with proper full cavitation developed. During this entire process, the forces, average and nonsteady, first increased and then decreased. The maximum average force and nonsteady force occurred at or near the condition of maximum oscillation in the cavity.

One cycle of the cavity oscillation is shown in Fig. 15. This figure shows the plan form of the developing cavitation at an angle of attack of 6 deg. The flow is left to right with the leading edge being at the left in both columns. The sequence starts at the upper left and time increases downward. These photographs are selected from a test filmstrip taken at 1200 frames per sec. Starting at the minimum cavity length, the cavity grows smoothly and, as it approaches the end of the hydrofoil, a reentrant jet is seen to form and gradually fill the rearward portion of the cavity. On reaching the end of the foil, the cavity surface becomes uneven and irregular and small vortices may be shed from the end of the cavity, causing small fluctuations in the force on the hydrofoil. The flow within the cavity then appears to become unstable and a large volume of cavity is abruptly shed into the stream; the cycle is then repeated. This sequence of events is similar to that of nonsteady cavitation reported by Knapp [6]. However, there are important differences: The cavity is not completely filled by the reentrant jet, although oscillations from incompletely filled cavities are reported by him. In the present case, and as can be seen in Fig. 15, there is always a cavity at the leading edge of the hydrofoil. The general stages of the oscillation are certainly very much as described by Knapp: "(*a*) Formation and growth, (*b*) filling, and (*c*) breakoff." The other difference in our view is that, when breakoff occurs, a large change in force ensues and there is a large corresponding change in circulation. This would lead one to suspect that the dynamics of the present phenomenon are related to the time-varying circulation.

The traces of the strain gage (to be discussed presently) were used to measure the frequency of the "strong" cavitation oscillations. These are shown for various angles of attack and tunnel velocities in Fig. 16. The frequencies are reported in terms of a dimensionless Strouhal number, chord times frequency over tunnel speed. The range of this parameter is from about 0.07 for a 4-deg angle of attack to about 0.14 at an 8-deg angle of attack. Although there is some variation with speed at the lowest angle, the reduced frequency is relatively constant at the highest angle. This would suggest that the frequency of oscillation is not strongly dependent on the rigidity of the surrounding tunnel structure. There is the basic question, however, of the effect of the tunnel and flow "compliance" on such transient cavity flows as described herein. For example, if the tunnel were perfectly rigid and if there were no free surface other than that of the cavity itself, then an infinite pressure difference (in an incompressible medium) would be required to create the changing cavity volume. The tunnel is compliant however; numerous pockets of vapor collect in the diffuser; and from the photographs in Figs. 7(*b*) to 10(*b*), it can be seen that there are entrained vapor-air bubbles in the flow. All of these effects evidently provide a cushion for the fluctuating cavity volume.

It is interesting to note that the frequencies observed by Knapp are much higher than those of the present work; in his work, they ranged from 51 to 200 cps. Calculations of the reduced frequency, based on the length of the cavity of these oscillations, are about twice the present values. Again, the reduced frequency of his observations is substantially independent of tunnel speed.

It was mentioned that the output of the strain gage was photographed on the motion-picture film such as shown in Fig. 15. Unfortunately, the trace was too dim to be reproduced in this

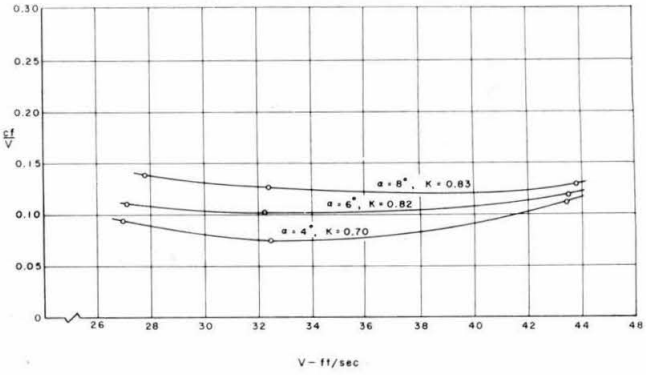

Fig. 16 Reduced frequency during phase of maximum force oscillations as a function of tunnel speed for varying angles of attack. Reynolds number range is from 0.62 × 10^6 to 1.05 × 10^6.

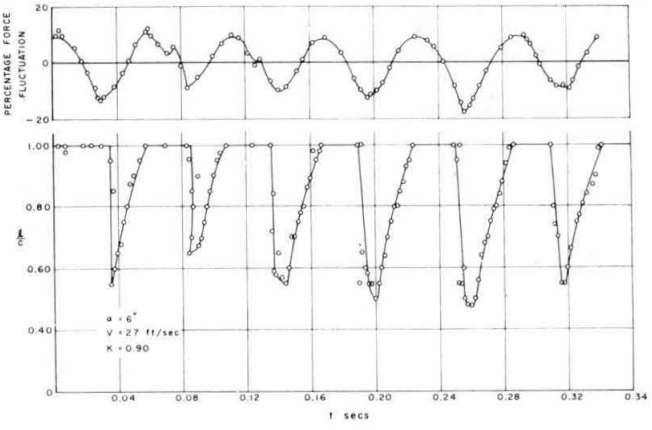

Fig. 17 Percentage force fluctuations and cavity length oscillation as a function of time in region of maximum oscillations for an angle of attack of 6 deg, tunnel speed of 27 fps, and cavitation number of 0.90

sequence of prints from the 16-mm film. Measurements could be made readily from the original film, however, by projecting the film frame by frame on a screen. By this means, measurements of force and cavity length were made, and a typical example of such a measurement is shown in Fig. 17. There it is seen that the double amplitude of the force oscillation is about 20 percent of the mean. The maximum force occurs at the maximum cavity length and the minimum force at the minimum cavity length. Generally speaking, there is no substantial phase change between the oscillations of cavity length and the oscillations of force. The lack of an appreciable phase change between the force and cavity oscillations suggests that possible inertial effects of the fluid in the tunnel circuit are not large, as has been indicated already, and that the tunnel boundaries are in effect not rigid.

Oscillograph recordings of the force are shown in Fig. 18 for one angle of attack (6 deg) and varying tunnel pressure at constant speed. The sequence of events previously described is borne out by this figure. For example, the high-frequency oscillations can just be discerned in the top trace; and as the pressure is lowered the small-amplitude fast oscillations develop. These lead into the characteristic large oscillation shown in the fourth trace. This trace is near the point of maximum oscillation and maximum lift force, as can be verified from Fig. 8. Finally, the oscillations die away with further reduction in pressure.

We have already mentioned the relative independence of reduced frequency upon tunnel speed for the large oscillations. The higher-frequency oscillations (the second and third traces in Fig. 18) are, however, more or less independent of tunnel speed. This raises the possibility that they are related to the dynamics of

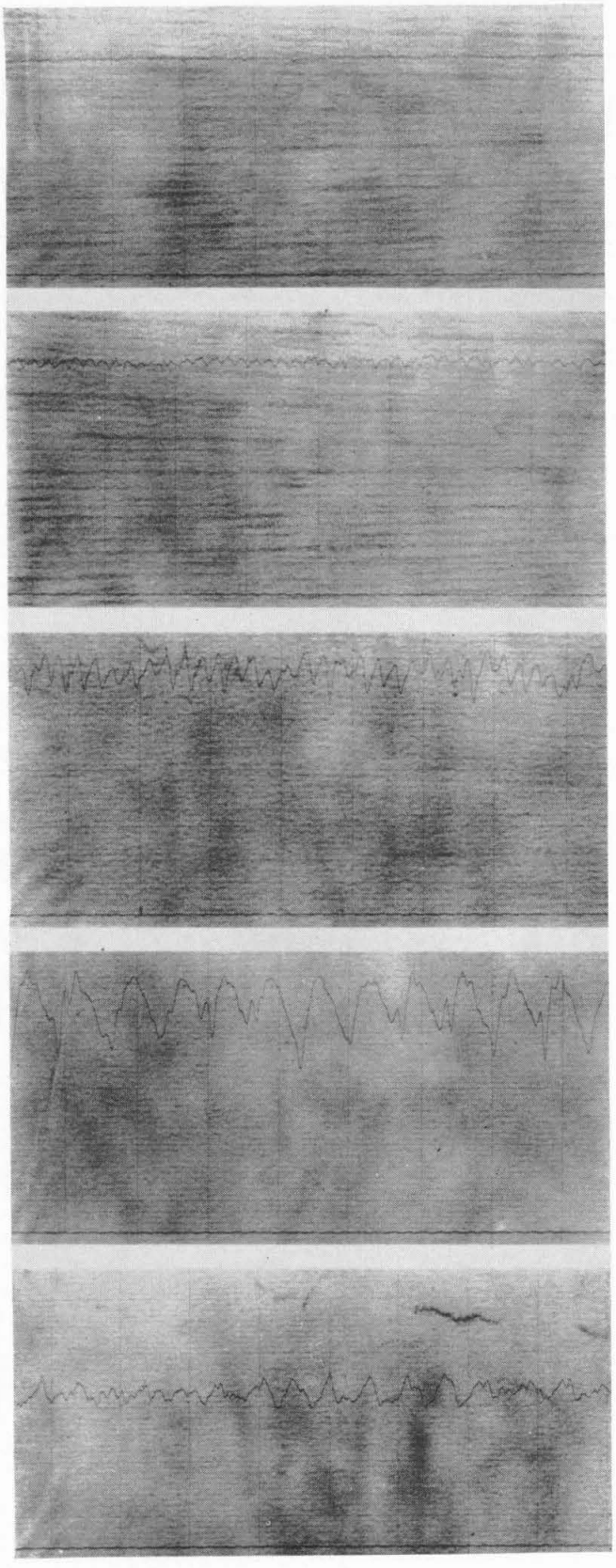

Fig. 18 Traces of oscillating force as recorded from strain-gage output as a function of time. Each time division represents 0.1 sec. Zero force datum is also illustrated at bottom of each trace. Tunnel speed is 31.4 fps at angle of attack of 6 deg. Sequence begins with top trace taken at a cavitation number of 1.69 and proceeds downward with corresponding cavitation numbers of 1.18, 1.03, 0.93, and 0.48. Point of maximum force oscillation is given by fourth trace.

the force balance or of the tunnel. To investigate this point, the force balance with model attached was shock-excited but no evidence of the 50–60 cps oscillations seen in Fig. 18 were observed. In fact, the lowest well-defined structural frequency observed was about 100 cps.

The unsteady cavitation behavior is by no means restricted to single hydrofoils. A similar phenomenon occurs in the case of cavitating cascades, as borne out by experiments recently carried out in the Hydrodynamics Laboratory. The series of events described here occurs again with little change qualitatively.

Conclusions

The characteristics of a plano-convex hydrofoil have been described for noncavitating and cavitating flows. It is found that the cavitation behavior can be divided into three regimes: A partially cavitating region, a fully cavitating region, and a region separating these two in which the flow is always unsteady.

In the partial and fully cavitating regions, the forces are steady and are well defined in terms of the cavitation number and angle of attack. In the unsteady zone, however, the forces fluctuate and the cavity oscillates violently. The fluctuating normal force on the hydrofoil measured in the present experiments has an amplitude variation of $\pm$ 10 percent of its mean value. The reduced frequency of the force oscillations appears to be a function principally of the angle of attack. Reduced frequencies based on chord length and tunnel velocity are in the range of 0.10 to 0.20 for angles of attack of 10 deg or less and for the tunnel velocities used. For the present tests, the cavity fluctuations are in phase with the force oscillations and the variation in cavity length is of the order of 60 percent of the chord.

The present investigations on the unsteady region of the cavitation on a hydrofoil are of a preliminary nature, the aim being to acquire some information on the processes involved and to obtain a general qualitative and quantitative picture of the unsteady phenomenon. Future work on the effects of tunnel boundaries and possible free surfaces are clearly necessary.

Acknowledgments

The participation of the members of the Hydrodynamics Laboratory staff, and in particular that of T. Kiceniuk, during the course of this experimental investigation is gratefully appreciated. This work was supported by the Department of the Navy under Contract Nonr 220(24).

References

1 J. Balhan, "Metingen aan Enige bij Scheepsschroeven Gerbruikelijke Profielen in Vlakke Stroming met en zonder Cavitatie," Nederlandse Scheepsbouwkundig Proefstation Te Wageningen, Publication No. 99, 1951.

2 O. Walchner, "Profilmessungen bei Kavitation," Hydromechanische Probleme des Schiffsantriebs, edited by G. Kempf and E. Foerster, Hamburg, 1932, pp. 256–267; English abstract, pp. 429–431.

3 R. W. Kermeen, "Water Tunnel Tests of NACA 4412 and Walchner Profile 7 Hydrofoils in Non-Cavitating and Cavitating Flows," Hydrodynamics Laboratory, California Institute of Technology, Pasadena, Calif., Report No. 47-5, 1956.

4 B. R. Parkin, "Experiments on Circular Arc and Flat Plate Hydrofoils in Non-Cavitating and Full Cavity Flows," Hydrodynamics Laboratory, California Institute of Technology, Pasadena, Calif., Report 47-6, 1956.

5 M. C. Meijer, "Some Experiments on Partly Cavitating Hydrofoils," *International Shipbuilding Progress*, vol. 6, no. 60, 1959, pp. 361–368.

6 R. T. Knapp, "Recent Investigations of the Mechanics of Cavitation and Cavitation Damage," TRANS. ASME, vol. 77, 1955, pp. 1045–1054.

7 R. T. Knapp, J. Levy, J. P. O'Neill, and F. B. Brown, "The Hydrodynamics Laboratory of the California Institute of Technology," TRANS. ASME, vol. 70, 1948, pp. 437–457.

8 G. M. Hotz and J. T. McGraw, "The High Speed Water Tunnel Three-Component Force Balance," Hydrodynamics Laboratory, California Institute of Technology, Pasadena, Calif., Report No. 47-2, 1955.

9 A. G. Fabula, "Choked Flow About Vented or Cavitating Hydrofoils," *Journal of Basic Engineering*, TRANS. ASME, Series D, vol. 86, 1964, pp. 561–568.

10 R. B. Wade, "Water Tunnel Observations on the Flow Past a Plano-Convex Hydrofoil," Hydrodynamics Laboratory, California Institute of Technology, Pasadena, Calif., Report No. E-79.6, February, 1964.

11 D. H. Williams, A. F. Brown, and C. J. W. Miles, "Tests on Four Circular-Back Aerofoils in the Compressed Air Tunnel," Aeronautical Research Council, Technical Report R and M, No. 2301, 1948.

12 G. B. McCullough and D. E. Gault, "Boundary Layer and Stalling Characteristics of the NACA 64A006 Airfoil Section," NACA TN 1923, 1949.

13 D. D. Carrow, "A Note on the Boundary Layer and Stalling Characteristics of Aerofoils," Aeronautical Research Council, CP No. 174, 1950.

14 T. Y. Wu, "A Note on the Linear and Non-Linear Theories for Fully Cavitating Hydrofoils," Hydrodynamics Laboratory, California Institute of Technology, Pasadena, Calif., Report No. 21–22, 1956.

15 A. J. Acosta, "A Note on Partial Cavitation of Flat Plate Hydrofoils," Hydrodynamics Laboratory, California Institute of Technology, Pasadena, Calif., Report No. E-19.9, 1955.

Printed in U. S. A.